Original Article

Mechanism of electroacupuncture at acupoints of the lung meridian through PKA/PKC regulation of TRPV1 in chronic cough after lung surgery in guinea pigs

Gao-Xiang Wang[1#^], Jie Zhou[2#], You-Mou Chen[3#], Liang-Dong Xu[1], Shan-Ming Tao[1], Jia Ma[3], Ye-Han Sun[3], Ming-Sheng Wu[1], Zheng-Wei Chen[1], Yong-Fu Zhu[3], Ming-Ran Xie[1]

[1]Department of Thoracic Surgery, The First Affiliated Hospital of USTC, Division of Life Sciences and Medicine, University of Science and Technology of China, Hefei, China; [2]Department of Acupuncture, The Third Affiliated Hospital of Zhejiang Chinese Medical University, Hangzhou, China; [3]The First Department of Oncology, The First Affiliated Hospital of Anhui University of Chinese Medicine, Hefei, China

Contributions: (I) Conception and design: GX Wang, YF Zhu, MR Xie; (II) Administrative support: J Zhou, YF Zhu, MR Xie; (III) Provision of study materials or patients: None; (IV) Collection and assembly of data: YM Chen, LD Xu, SM Tao, J Ma; (V) Data analysis and interpretation: YH Sun, MS Wu, ZW Chen; (VI) Manuscript writing: All authors; (VII) Final approval of manuscript: All authors.

[#]These authors contributed equally to this work.

Correspondence to: Ming-Ran Xie, MD, PhD. Department of Thoracic Surgery, The First Affiliated Hospital of USTC, Division of Life Sciences and Medicine, University of Science and Technology of China, Lujiang Road No. 17, Hefei 230001, China. Email: xmr1981@ustc.edu.cn; Yong-Fu Zhu, MD. The First Department of Oncology, The First Affiliated Hospital of Anhui University of Chinese Medicine, Meishan Road No. 117, Hefei 230031, China. Email: zyf240@ahtcm.edu.cn.

Background: Acupuncture has achieved good results in the treatment of cough, asthma, chronic obstructive pulmonary disease (COPD) and other lung diseases, but the mechanism associated with acupuncture in the treatment of chronic cough induced by lung surgery is unknown. We investigated whether acupuncture therapy could improve the symptoms of chronic cough after lung surgery through cyclic-AMp dependent protein kinase A (PKA)/cyclic-AMp dependent protein kinase C (PKC) regulation of the transient receptor potential vanilloid-1 (TRPV1) signaling pathway.

Methods: The guinea pigs were divided into 5 groups: the Sham operation Group (Sham), the Model Group (Model), the Electroacupuncture + Model Group (EA + M), the H89 + Model Group (H89 + M) and the Go6983 + Model Group (Go6983 + M). The effect of treatment was determined by measuring cough symptoms (number of coughs/cough incubation period) as the outcome criterion. The levels of inflammatory cytokines in bronchoalveolar lavage fluid (BALF) and blood were determined by enzyme-linked immunosorbent assays (ELISA). Lung tissue was stained with hematoxylin and eosin (H&E). The expression of p-PKA, p-PKC and p-TRPV1 proteins was measured by Western blotting. The mRNA levels of TRPV1, Substance P (SP), calcitonin gene-related peptide (CGRP) and neurokinin-1R (NK1R) were measured by real-time polymerase chain reaction (RT-PCR).

Results: Acupuncture significantly reduced the cough frequency and prolonged the cough latency of chronic cough in guinea pigs after lung surgery. In addition, acupuncture reduced the damage to lung tissue. The levels of inflammatory cytokines decreased in all treatment groups, the expression levels of p-PKA, p-PKC and p-TRPV1 were significantly inhibited and the mRNA levels of TRPV1, SP, CGRP and NK1R decreased significantly after acupuncture treatment.

Conclusions: Acupuncture therapy ameliorated chronic cough in guinea pigs after lung surgery by regulating the TRPV1 signaling pathway via PKA/PKC. Our results showed that acupuncture may be an effective treatment of chronic cough after lung surgery, and also clarified the potential mechanism, which provides a theoretical basis for the clinical treatment of patients with chronic cough after lung surgery.

Keywords: Cough; electroacupuncture; lungs; transient receptor potential vanilloid-1 (TRPV1)

^ ORCID: 0000-0001-9445-0501.

Submitted Jan 10, 2023. Accepted for publication Apr 21, 2023. Published online Apr 28, 2023.
doi: 10.21037/jtd-23-409
View this article at: https://dx.doi.org/10.21037/jtd-23-409

Introduction

With the recent progress in imaging technology and the popularization of low-dose spiral computed tomography, an increasing number of patients have been clinically identified with pulmonary nodules, some of which have been identified as early non-small cell lung cancer after surgery (1,2). However, some patients develop acute or chronic cough symptoms after lung surgery, with a deleterious effect on their quality of life (3-5).

Cough is a common symptom of respiratory disease and the most important respiratory defense reflex. The related afferent nerves affecting the airway reflex mainly include myelinated Aδ fibers, which are sensitive to various mechanical stimuli, and unmyelinated C fibers, which are sensitive to various types of chemical stimuli (6,7). The C-fiber nerve endings of the lung contain TRPV1, and various physical and chemical stimuli can activate TRPV1-induced cough (8-10). Our previous study found that among patients undergoing lung surgery, those diagnosed with postoperative acute or chronic cough had significantly higher levels of serum prostaglandin E2 (PGE2) and bradykinin (BK; the upstream protein of TRPV1) (11). Therefore, we believe that PGE2 and BK increase respiratory inflammation and trigger an increase in cough by activating the TRPV1 pathway. Other studies have reported that PGE2 and BK cause conscious animal and human coughs when inhaled in aerosol form, and patients taking angiotensin converting enzyme inhibitors also develop excessive coughing due to reduced decomposition of BK (12-14). Therefore, we believe that intervention in the TRPV1 pathway and reduction in airway inflammation can prevent and reduce chronic cough after lung surgery. Revealing the pathogenesis of postoperative cough symptoms and its effective treatment has important theoretical implications and practical clinical significance.

Acupuncture is an important part of Traditional Chinese Medicine (15,16). It has been reported that acupuncture can reduce the postoperative inflammatory response in patients undergoing lung surgery, thus reducing postoperative pulmonary complications such as cough (17,18). In addition, clinical studies have confirmed that acupuncture can achieve good results in the treatment of cough, asthma, chronic obstructive pulmonary disease (COPD) and other lung diseases (19-21). However, the mechanism of acupuncture in the treatment of chronic cough caused by pulmonary surgery is unknown. Therefore, in the present study, a model of chronic cough after lung operation in guinea pigs was established, and electroacupuncture at acupoints of the lung meridian, the protein kinase A (PKA) inhibitor H89 and the protein kinase C (PKC) inhibitor Go6983 were used to confirm that acupuncture of the lung meridian regulates TRPV1 through PKA/PKC. PKA/PKC could activate TRPV1 to induce cough. Changes in cough frequency and lung histopathology were observed in different groups of guinea pigs with chronic cough after lung surgery. The airway inflammation indexes of the chronic cough model after lung surgery were evaluated, and the protein expression levels of PGE2, BK, TRPV1, p-PKA, p-PKC and p-TRPV1 were measured. The TRPV1, SP, CGRP and NK1R mRNA levels in the lung tissue of guinea pigs were measured by real-time fluorescence quantitative polymerase chain reaction (PCR). We present the following article in accordance with the ARRIVE reporting checklist (available at https://jtd.amegroups.com/article/view/10.21037/jtd-23-409/rc).

Highlight box

Key findings

- Acupuncture therapy ameliorated chronic cough in guinea pigs after lung surgery by regulating the TRPV 1 signaling pathway via PKA/PKC.

What is known and what is new?

- TRPV 1 controls cough.
- Acupuncture can regulate TRPV 1 by PKA/PKC to treat chronic cough.

What is the implication, and what should change now?

- Acupuncture can treat chronic cough.

Methods

Experimental materials

A guinea pig PGE2 enzyme-linked immunosorbent assay (ELISA) kit and BK ELISA kit were purchased from Elabscience Biotechnology Co., Ltd. (Wuhan, China).

The TRPV1 ELISA kit was purchased from Cloud-Clone Corp. (formerly Uscn Life Science Inc., Wuhan, China). TRIzol was purchased from Ambion Inc. (Austin, TX, USA). HiScript Reverse Transcriptase (RNase H), 5 × HiScript Buffer and SYBR Green Master Mix were purchased from Vazyme (Nanjing, China). DNTP, Taq Plus DNA Polymerase and DL2000 DNA Marker were purchased from the TIANGEN Company (Beijing, China). Random Primer (N6) was purchased from Takara Bio USA, Inc. (San Jose, CA, USA). Concentrated normal goat serum (closed), fluorescent labeled sheep anti-rabbit IgG and horseradish peroxidase (HRP)-labeled sheep anti-rabbit secondary antibody were purchased from China Wuhan Boshi Bioengineering Co., Ltd. (Wuhan, China). DAPI, phosphatase inhibitor, PMSF, RIPA lysate and BCA protein concentration determination kits were purchased from Beijing Biyuntian Company (Beijing, China). The anti-fluorescence quenching tablet was purchased from SouthernBiotech (Birmingham, AL, USA). P-TRPV1 (rabbit), p-PKA (rabbit) and p-PKC (rabbit) were purchased from Affinity Company (San Francisco, CA, USA). The protein marker (10–250 kD) was purchased from Fermentas (Waltham, MA, USA). PVDF film (0.45 μm) was purchased from Millipore (Burlington, MA, USA). Rabbit multi-antibody GAPDH (37 KD) was purchased from Hangzhou Xianzhi Shengwu Co., Ltd., China (Hangzhou, China). p-PKC (rabbit) (77 kD), p-PKA (rabbit) (41 kD) and P-TRPV1 (rabbit) (95 kD) were purchased from Affinity Company, USA. ECL substrate liquid was purchased from Thermo Scientific, USAs. Hematoxylin was purchased from Sigma, Germany. Water-soluble eosin Y, xylene, embedded paraffin and neutral gum were purchased from China National Pharmaceutical Group Corporation. Capsaicin was purchased from Beijing Solarbio Biotechnology Co., Ltd. (Beijing, China).

Experimental animal model

The study animals comprised 40 healthy adult male Dunkin-Hartley guinea pigs aged 5–7 weeks and weighing 300–350 g (Experimental Animal Center of Anhui University of Chinese Medicine; License No. Wan SCXK2017-001). Excluding those that died or were injured during feeding, finally 30 guinea pigs were included in the study. The guinea pigs were housed in a specific pathogen-free environment with a temperature of 20–26 ℃, daily temperature fluctuation ≤4 ℃ and a humidity of 40–70%. The light/dark cycle was 12 h and the animals had free access to food and water. A protocol was prepared before the study without registration. Animal experiments were performed under a project license (No. AHUCM-mouse-2022059) granted by the ethics board of Anhui University of Chinese Medicine, in compliance with institutional guidelines for the care and use of animals.

Grouping of experimental animals

After 1 week of acclimation, all guinea pigs were randomly divided into 5 groups (n=6): Sham Group (Sham), Model Group (Model), Electroacupuncture + Model Group (EA + M), H89 + Model Group (H89 + M) and Go6983 + Model Group (Go6983 + M). We followed Zhu *et al.* in the establishment of the animal experimental model (22).

According to the results of our previous study, referring to the route of human meridians, combined with the acupuncture and moxibustion acupoint positioning standard of Chinese Veterinary Acupuncture and moxibustion on guinea pigs, based on the literature (23). Two Φ 0.30×25 mm filigree needles were used and connected to an SDZ-IV type electronic acupuncture apparatus with the following stimulation parameters: the current (IP-P) was 1 mA, the frequency was 2 Hz, and electroacupuncture was performed continuously for 30 min. The stimulation parameters were the same for each group. Acupuncture intervention lasted for 1 week. The guinea pigs in the inhibitor groups were given intraperitoneal injections of H89 and Go6983 (injection doses of 20 mg/kg and 22 μg/kg, respectively) for the 1 week of intervention. The experimental schedule is shown in *Figure 1*.

Experimental protocol

Monitoring of the number of coughs in guinea pigs

The whole body plethysmography system (WBP, Shanghai TOW Intelligent Technology Co., Ltd., Shanghai, China) was used to determine the number of coughs. The guinea pigs in each group were placed in the transparent chamber of the WBP and allowed to move freely for 6 min while the number of coughs was recorded. The guinea pigs were considered to be coughing based on characteristic body positions, such as opening their mouths, extending their front feet and necks forward (24,25). Cough counts were recorded and analyzed by two trained observers.

Histological evaluation

Lung tissue was sectioned (4 μm), deparaffinized, and dehydrated in decreasing concentrations of ethanol,

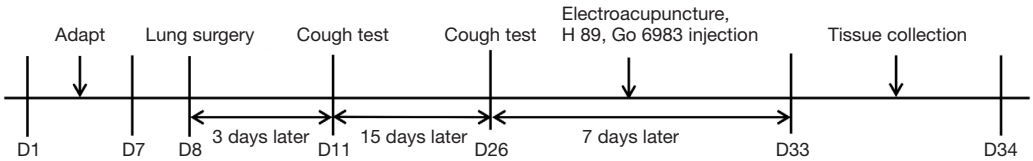

Figure 1 Experimental timeline.

followed by rinsing with distilled water and staining with hematoxylin and eosin (H&E). Microscopic images of stained sections were obtained at ×100 magnification.

ELISA

The levels of PGE2, BK, and TRPV1 protein expression in bronchoalveolar BALF supernatant and blood were determined using ELISA kits according to the manufacturers' instructions.

Western blotting

Total protein of the lung tissue was extracted according to the instructions of RIPA lysis buffer, and the BCA method was used to prepare protein samples. The prepared protein samples and MAKER were added to sample wells with a micropipette, and the total protein content of each sample was 40 μg. After adding the sample, electrophoresis was run at a constant current of 80 V until the bromophenol blue indicator became a line at the junction of the concentrating and separating gels, and a constant current of 120 V brought bromophenol blue to the bottom of the sample. The target protein was transferred to a PVDF membrane and blocked with 5% nonfat milk powder for 2 h. After washing, the PVDF membranes were immersed in primary antibody and incubated overnight at 4 ℃. The next day, the corresponding HRP-labeled secondary antibody was diluted with blocking solution at 1:50,000, and the PVDF membrane was immersed in the secondary antibody solution and incubated at 37 ℃ for 2 h on a shaker. The enhanced solution in the electrochemoluminescent reagent was mixed with stabilized peroxidase solution at a ratio of 1:1, the working solution was dropped onto the PVDF membrane, the membrane was allowed to react for a few minutes, and the fluorescence band appeared. The film was then cleaned, dried, scanned, and then analyzed for greyscale values using IPP (Image Pro-Plus).

Real-time fluorescence quantitative PCR

A small amount lung tissue was frozen with liquid nitrogen and stored in a 1.5-mL Eppendorf tube. TRIzol reagent (1 mL) was added to extract RNA. OD260, OD280 and OD260/OD280 were measured by microspectrophotometer to calculate the purity and concentration of RNA. cDNA was synthesized according to the instructions of the reverse transcription kit. The related mRNA was amplified by PCR, and the total reaction volume was 20 μL. The primer sequence is given in Table S1. The reaction conditions were as follows: predenaturation at 95 ℃ and annealing at 60 ℃ for 30 s, repeated for 40 cycles. The relative gene expression was calculated by the $2^{-\Delta\Delta Ct}$ method.

Statistical analysis

All the data in the experiment are expressed as the mean ± standard deviation (mean ± SD). The fluorescence area of each group was analyzed by ImageJ software. Statistical analysis was carried out with GraphPad Prism 6 software. One-way ANOVA was used to compare the mean and multiple groups, the Bonferroni test was used to compare groups, and Spearman linear correlation analysis was used to test the correlation. R squared was recorded as R^2. $P<0.05$ indicated that the difference was statistically significant.

Results

Monitoring cough in experimental groups

The cough frequency (times/6 min) was 2.50±0.54 in the Sham Group, 15.67±1.63 in the Model Group, 7.50±2.88 in the EA + M Group, 9.17±1.17 in the H89 + M Group and 9.50±1.05 in the Go6983 + M Group. There was a significant difference between the Model Group and the EA + M, H89 + M and Go6983 + M groups ($P<0.05$, *Figure 2*). The specific P values are given in Table S2.

Pathological results in experimental group

Lung tissue was collected from guinea pigs in each group (*Figure 3*) and compared. In the Sham Group, the lung tissue appeared normal whereas in the EA + M, H89 +

M and Go6983 + M groups the lung epithelial cells were swollen and degenerated to varying degrees, accompanied by varying degrees of inflammatory cell infiltration. The Model Group had more severe pathological lung damage, and extensive inflammatory cell infiltration. Compared with the H89 + M and Go6983 + M groups, the EA + M Group showed alleviated lung damage.

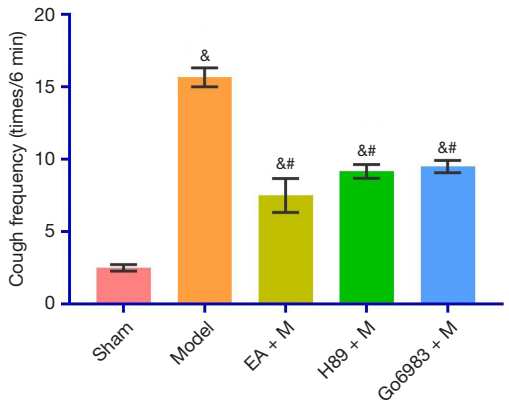

Figure 2 Changes of cough in each group after intervention. [&], Sham Group compared with the other groups, P<0.05. [#], Model Group compared with the other groups, P<0.05. EA, electroacupuncture; M, Model.

ELISA detection of changes in PGE2, BK, and TRPV1 protein expression and correlation analysis in the BALF and blood of guinea pigs in each group

The levels of PGE2, BK and TRPV1 protein in the BALF from the Sham Group were significantly different from those in the Model Group, and there were significant differences between the Model Group and the EA + M, H89 + M and Go6983 + M groups (P<0.05, *Figure 4*). There were no significant differences among the EA + M, H89 + M and Go6983 + M groups (P>0.05, *Figure 4*; specific P values are given in Table S3). Chronic cough after pneumonectomy in the guinea pigs positively correlated with the expression of PGE2, BK and TRPV1 in BALF (Figure S1).

Quantitative analysis of p-PKA, p-PKC and p-TRPV1 protein expressions and correlation in lung tissue of guinea pigs by Western blotting

Compared with the Sham Group, the protein expression of p-PKA in the lung tissue of the chronic cough Model Group after lung surgery was significantly increased on the 15th day of modeling (P<0.05); compared with the Model Group, the expression of p-PKA protein in the lung

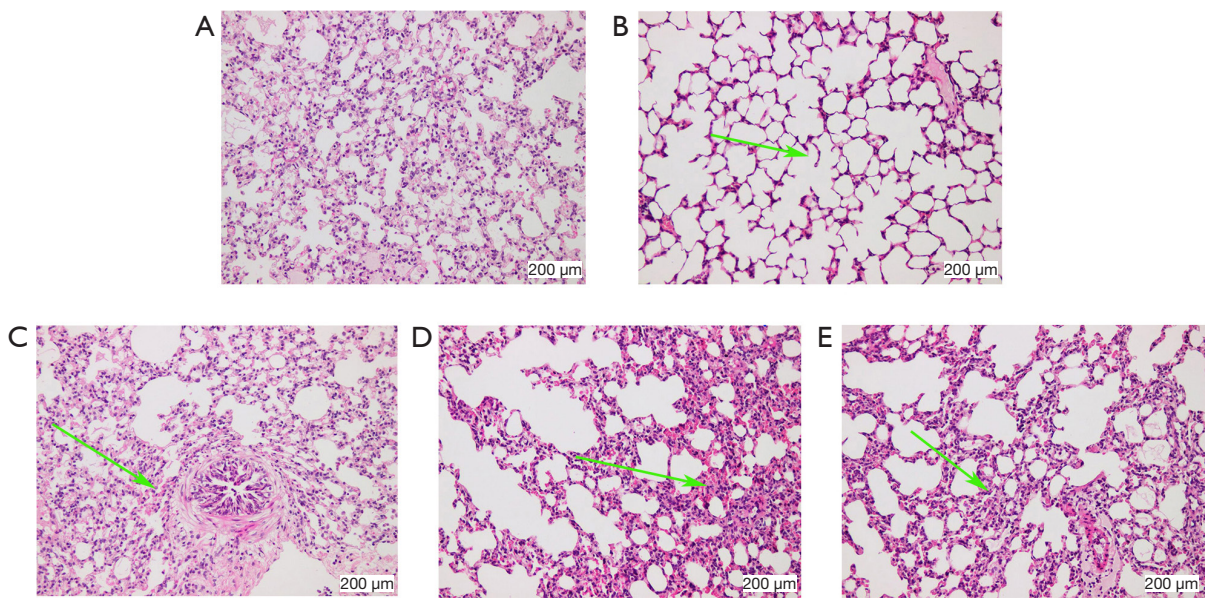

Figure 3 Pathological changes of guinea pig lung tissue (hematoxylin and eosin staining). (A) Sham Group, (B) Model Group, (C) EA + Model Group, (D) H89 + Model Group, (E) Go6983 + Model Group. Arrows represent swelling, degeneration or inflammatory cell infiltration of lung epithelial cells. A, electroacupuncture; M, Model.

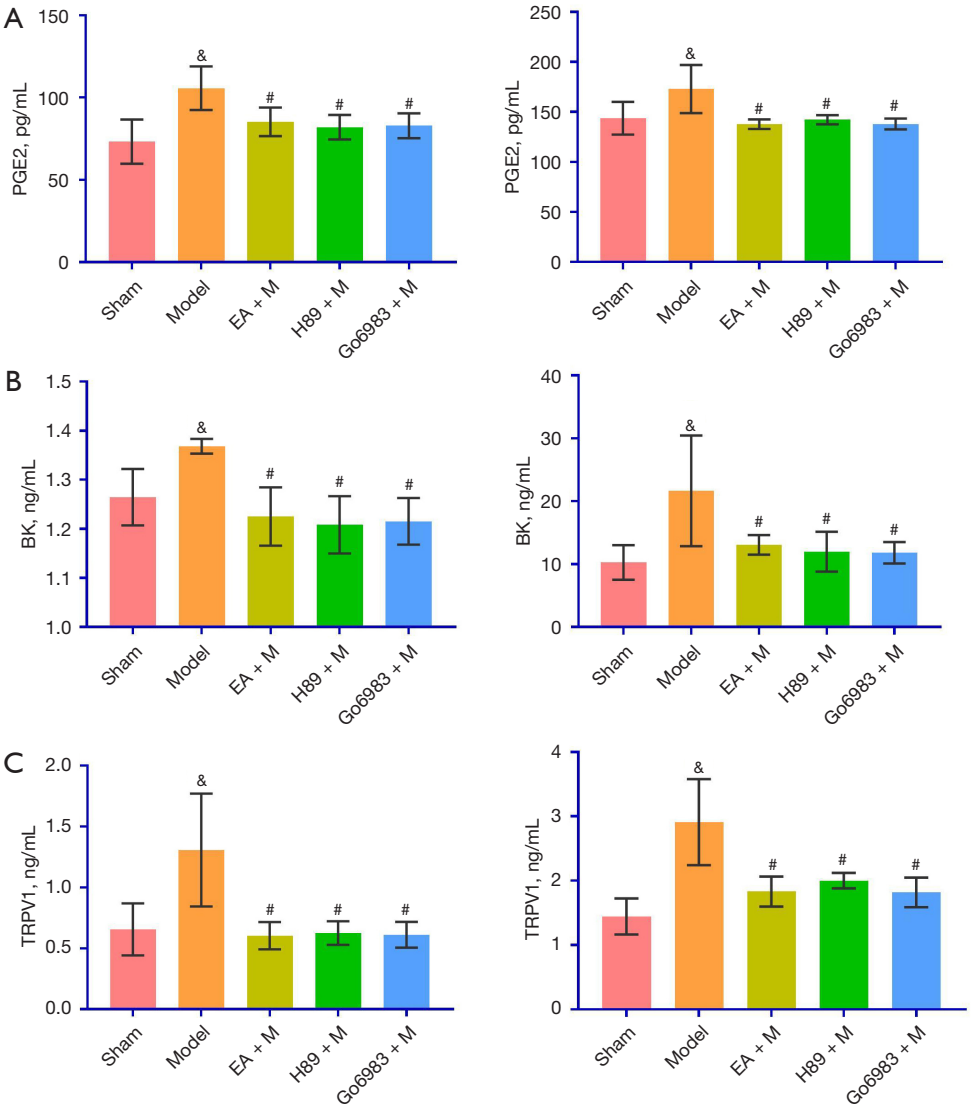

Figure 4 Bronchoalveolar lavage fluid and blood analysis of PGE2, BK and TRPV1 protein expression changes in each group of guinea pigs. [&], Sham Group compared with the other groups, P<0.05; [#], Model Group compared with the other groups, P<0.05. EA, electroacupuncture; M, Model; PGE2, prostaglandin E2; BK, bradykinin; TRPV1, transient receptor potential vanilloid-1.

tissue of the EA + M Group and the H89 + M Group was significantly decreased (P<0.05); compared with the EA + M Group, the expression of p-PKA protein in the H89 + M Group was significantly decreased (P<0.05), as shown in *Figure 5* (Table S4 for P values.) According to p-PKA protein expression in lung tissue, chronic cough after lung resection in guinea pigs positively correlated with PKA (R^2=0.2828, P<0.05, *Figure 5*).

Compared with the Sham Group, the protein expression of p-PKC in the lung tissue of the Model Group on the 15th day of modeling was significantly increased (P<0.05). Compared with the EA + M Group, the p-PKC protein expression of the Go6983 + M Group decreased significantly (P<0.05), as shown in *Figure 5* (specific P values are given in Table S4). According to p-PKC protein expression in lung tissue, chronic cough after lung resection in guinea pigs positively correlated with p-PKC (R^2=0.2038, P<0.05, *Figure 5*).

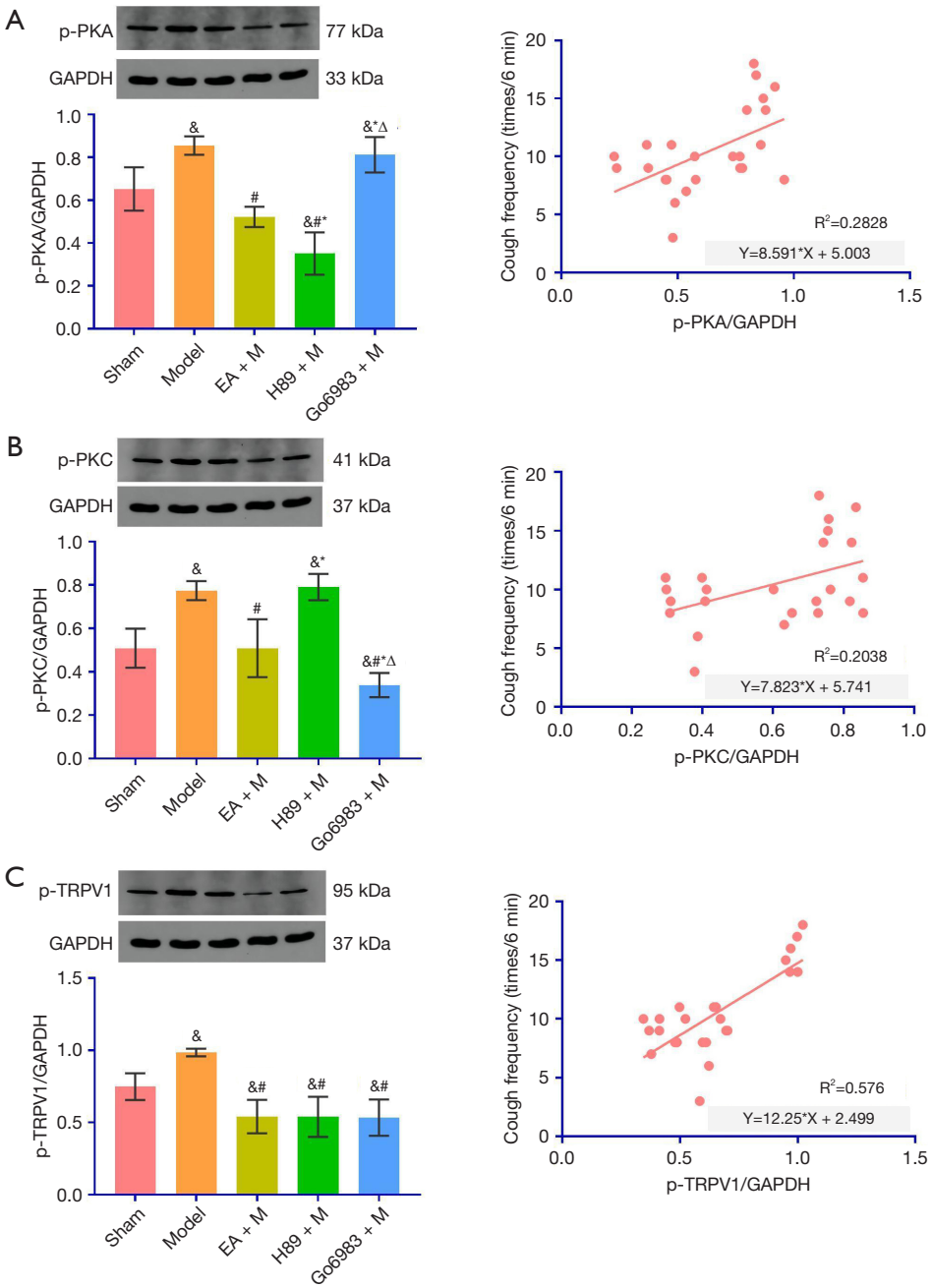

Figure 5 Western blot quantitative analysis of p-PKA, p-PKC and p-TRPV1 in guinea pig lung. [&], Sham Group compared with the other groups, P<0.05. [#], Model Group compared with the other groups, P<0.05. *, EA + M Group compared with the other groups, P<0.05. [Δ], H89 + M Group compared with the other groups, P<0.05. EA, electroacupuncture; M, Model; PKA, protein kinase A; PKC, protein kinase C; TRPV, transient receptor potential vanilloid.

Compared with that in the Sham Group, the protein expression of p-TRPV1 in the lung tissue of the chronic cough Model Group after lung surgery was significantly increased on the 15th day of modeling (P<0.05). The expression of p-TRPV1 protein in the lung tissue of the H89 + M Group and the Go6983 + M Group was significantly decreased (P<0.05), as shown in *Figure 5*, and the specific P values are shown in Table S4. According to p-TRPV1 protein expression in lung tissue, chronic cough after lung resection in guinea pigs positively correlated with p-TRPV1, R^2=0.5760, P<0.05, *Figure 5*.

Measurement of TRPV1, SP, CGRP and NK1R mRNA in lung tissue of guinea pigs by real-time fluorescence quantitative PCR and correlation analysis

Real-time quantitative PCR was used to measure the TRPV1 mRNA content in guinea pig lung tissue. Compared with the Sham, EA + M, H89 + M and Go6983 + M groups, the Model Group showed a significant difference (P<0.05). Compared with the H89 + M Group, the EA + M Group had no statistical significance (P>0.05). Compared with the Go6983 + M Group, the EA + M Group showed a significant difference (P<0.05, *Figure 6*; specific P value is shown in Table S5). The level of TRPV1 mRNA in lung tissue positively correlated with chronic cough after pneumonectomy in guinea pigs (R^2=0.3023, P<0.05, *Figure 6*).

Real-time quantitative PCR was used to detect the SP (Substance P) mRNA content in guinea pig lung tissue. Compared with the Sham Group, EA + M Group, H89 + M Group and Go6983 + M Group, there was a significant difference in the Model Group (P<0.05). Comparing the EA + M, H89 + M and Go6983 + M groups, there was no statistical significance (P>0.05) (*Figure 6*; specific P value is shown in Table S5). Regarding the level of SP mRNA in lung tissue, chronic cough after pneumonectomy in guinea pigs positively correlated with SP (R^2=0.5344, P<0.05, *Figure 6*).

Real-time quantitative PCR was used to measure CGRP (calcitonin gene-related peptide) mRNA content in guinea pig lung tissue. Compared with the Sham, EA + M, H89 + M and Go6983 + M groups, there was a significant difference in the Model Group (P<0.05). Compared with the H89 + M Group, the EA + M Group had no significant difference (P>0.05). Compared with the H89 + M and Go6983 + M groups, the EA + M Group showed a significant difference (P<0.05, *Figure 6*; specific P value is shown in Table S5). Based on the level of CGRP mRNA in lung tissue, chronic cough after pneumonectomy in guinea pigs positively correlated with CGRP (R^2=0.3339, P<0.05, *Figure 6*).

Real-time quantitative PCR was used to measure NK1R mRNA content in guinea pig lung tissue. Compared with the Sham, EA + M, H89 + M and Go6983 + M groups, there was a significant difference in the Model Group (P<0.05). Comparing the EA + M, H89 + M and Go6983 + M groups, there was no significant difference (P>0.05, *Figure 6*; specific P value is shown in Table S5). Based on the level of NK1R mRNA in lung tissue, chronic cough positively correlated with NK1R after pneumonectomy in guinea pigs (R^2=0.4549, P<0.05, *Figure 6*).

Discussion

Lung surgery can induce cough and if present for more than 8 weeks it is defined as chronic. Cough is not only a physiological response to airway stimulation but is also related to the lymph node dissection area, surgical site, surgical method, and protective effect on healthy lungs during surgery (26-28). Cough is also one of the most common symptoms of respiratory diseases. Although it is a protective reflex, long-term coughing seriously affects quality of life.

Airway inflammation an important pathological mechanism of cough and is divided into infectious, allergic and neurogenic (29,30). The different types of inflammation may occur simultaneously. Various physical and chemical factors will stimulate the respiratory system after lung surgery, such as local pleurisy and pleural effusion, chronic irritation caused by surgical scars and foreign bodies, and postoperative airway irritation.

Acupuncture is an integral part of Traditional Chinese Medicine and can enhance the functioning of the patient's immune system, thereby reducing phlegm and inflammation (31). According to a number of clinical reports, acupuncture and moxibustion have achieved good results in the treatment of cough, asthma, COPD and other lung diseases (19-21). For patients with poor drug treatment effect, you can try acupuncture treatment. Acupuncture treatment makes cough treatment methods diversified. In the present study using an animal model of postoperative cough, we found that the number of coughs within 6 min in the EA + M, H89 + M and Go6983 + M groups was significantly lower than that in the Model

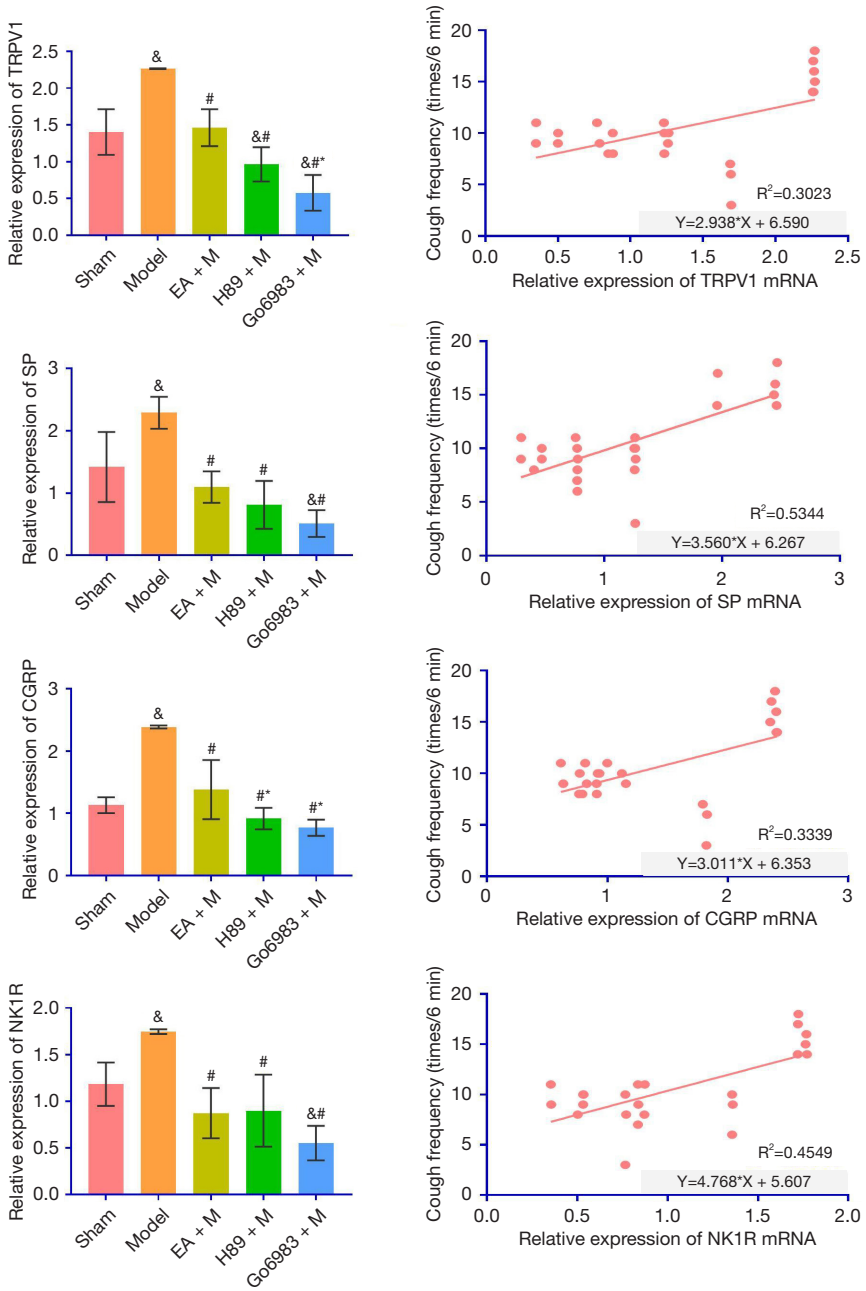

Figure 6 Real-time fluorescence quantitative PCR analysis of TRPV1, SP, CGRP and NK1R mRNA in guinea pig lungs. [&], Sham Group compared with the other groups, P<0.05. [#], Model Group compared with the other groups, P<0.05. *, EA + M Group compared with the other groups, P<0.05. EA, electroacupuncture; M, Model; PCR, polymerase chain reaction; SP, substance P; NK1R, neurokinin-1R; CGRP, calcitonin gene-related peptide; TRPV1, transient receptor potential vanilloid-1.

Group. In addition, the results of pathological investigations showed that the pulmonary epithelial cells in the EA + M, H89 + M and Go6983 + M groups were swollen and variously degenerated, accompanied by different degrees of inflammatory cell infiltration. In the Model Group, the lung pathological damage was more serious, with many infiltrated inflammatory cells. Compared with the H89 + M and Go6983 + M groups, the pathological lung damage in the EA + M Group was alleviated. Electroacupuncture at acupoints of the lung meridian and application of the inhibitors H89 and Go6983 alleviated the cough symptoms of these guinea pigs after pneumonectomy.

In our previous study (11), we found that the postoperative serum PGE2, BK and TRPV1 levels in 60 patients who underwent lung surgery were significantly higher than before surgery. Of them, 22 developed chronic cough, and 25 were diagnosed with non-chronic cough. The serum levels of PGE2, BK and TRPV1 in the chronic cough group were significantly higher than those in the non-chronic cough group at 8 weeks after surgery. As endogenous inflammatory mediators, PGE2 and BK activate the TRPV1 pathway by activating G protein-coupled receptors, increasing airway inflammation and triggering cough. Grace *et al.* found that the TRPV1 blockade in the guinea pig cough model inhibited the cough response of PGE2 and BK, and that the TRPV1 pathway was a key regulator of the cough response (32). In the present study, by comparing the results of BALF and blood ELISA to analyze the changes in the expression of PGE2 and BK in the guinea pigs in each group, we found that the expression of PGE2 and BK in the chronic cough Model Group was significantly increased after lung surgery. The expression levels of PGE2 and BK proteins in the acupuncture group were significantly decreased. Therefore, it can be inferred that electroacupuncture intervention can inhibit TRPV1 by reducing the expression of PGE2 and BK.

H89 is a commonly used inhibitor that can selectively inhibit a variety of protein kinases (including PKA, PKC and PKD, where PKA and PKD are involved in the control of Golgi morphology), but it has a stronger selective inhibitory effect on PKA (33,34). The inhibitor Go6983 is a classic PKC inhibitor. Ma *et al.* showed that PGE2 agonist-induced TRPV1 activation can be inhibited by PKA inhibitors (35). In addition, we found that the protein levels of p-PKA, p-PKC and p-TRPV1 in the chronic cough Model Group increased significantly after lung surgery. The protein levels of p-PKA, p-PKC and p-TRPV 1 in the electroacupuncture group was significantly reduced compared with the Model Group after electroacupuncture treatment. The protein content of p-PKA in guinea pigs treated with the inhibitor H89 was significantly lower than in the Model Group, and the protein content of p-PKC in guinea pigs treated with the inhibitor Go6983 was significantly lower than that in the Model Group. Therefore, we speculate that acupuncture can treat chronic cough by reducing PGE2 and BK through intervening in the PKA and PKC pathways to activate the *TRPV1* gene to secrete TRPV1 protein.

Activation of TRPV1 ion channels leads to calcium influx into nerve terminals (33). The current concept is that the TRPV1 receptor acts as a "switch" for coughing. An airborne irritant that enters the lungs activates sensory nerves after contact with receptors, leading to a series of responses that manifest as coughing. In addition, studies have confirmed that TRPV1 can affect the release of neuropeptide substances (SP, CGRP and NK1R, etc.) (36,37). Our study found that the expression of SP, CGRP, and NK1R mRNA in the chronic cough Model Group was significantly increased after lung surgery, and the expression of SP, CGRP, and NK1R mRNA was significantly decreased after electroacupuncture at acupoints of the lung meridian and application of the inhibitors H89 and Go6983. These findings suggest that TRPV1 can interfere with the expression of SP, CGRP, NK1R and other neuropeptide proteins to cause chronic cough after lung surgery.

Conclusions

Electroacupuncture of the lung meridian reduced the number of coughs and the infiltration of inflammatory cells in a guinea pig model of chronic cough after lung surgery. In addition, electroacupuncture in the lung meridian inhibited the expression and secretion of SP, CGRP and NKA and reduced the infiltration of inflammatory cells by reducing the expression of the p-PKA and p-PKC-activated *TRPV1* gene by interfering with PEG2 and BK (*Figure* 7). These findings provide new insights into the treatment of postoperative chronic cough.

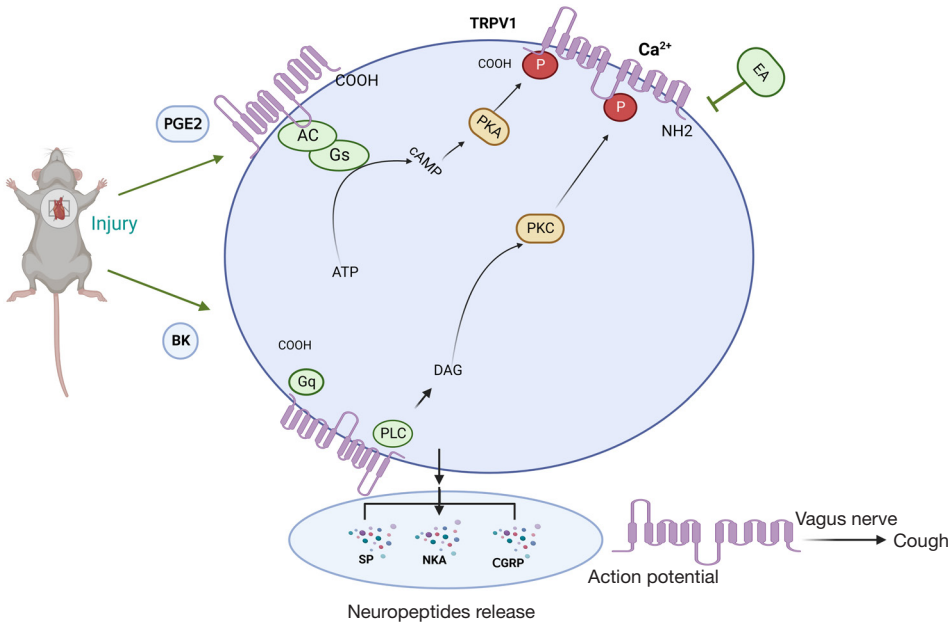

Figure 7 Hypothesis diagram. PGE2, prostaglandin-E2; CGRP, calcitonin gene-related peptide; NKA, neurokinin A; SP, substance P; TRPV1, transient receptor potential vanilloid 1; PKA, cyclic-AMp dependent protein kinase A; PKC, cyclic-AMp dependent protein kinase C; EA, electroacupuncture; BK, bradykinin capsaicin.

Acknowledgments

Funding: This work was supported by grants from the Opening Project of Zhejiang Provincial Preponderant and Characteristic Subject of Key University (Chinese Traditional Medicine), Zhejiang Chinese Medical University (No. ZYXZD2019004); the National Natural Science Foundation of China (No. 81973643), the Key Projects of Natural Science Research in Anhui Universities in 2021 (No. KJ2021A0557); the Fundamental Research Funds for the Central Universities (No. WK9110000021); Key research and development projects in Anhui Province (No. 202004j07020017); Anhui Health Research Project in 2022 (No. AHWJ2022b053); Exploration project of Xin'an Physicians' Thoughts on Treating Tumor and Its Syndromes (No. 2022AH050415).

Footnote

Reporting Checklist: The authors have completed the ARRIVE reporting checklist. Available at https://jtd.amegroups.com/article/view/10.21037/jtd-23-409/rc

Data Sharing Statement: Available at https://jtd.amegroups.com/article/view/10.21037/jtd-23-409/dss

Peer Review File: Available at https://jtd.amegroups.com/article/view/10.21037/jtd-23-409/prf

Conflicts of Interest: All authors have completed the ICMJE uniform disclosure form (available at https://jtd.amegroups.com/article/view/10.21037/jtd-23-409/coif). The authors have no conflicts of interest to declare.

Ethical Statement: The authors are accountable for all aspects of the work in ensuring that questions related to the accuracy or integrity of any part of the work are appropriately investigated and resolved. Animal experiments were performed under a project license (No. AHUCM-mouse-2022059) granted by ethics board of Anhui University of Chinese Medicine, in compliance with institutional guidelines for the care and use of animals.

References

1. Siegel RL, Miller KD, Fuchs HE, et al. Cancer Statistics, 2021. CA Cancer J Clin 2021;71:7-33.
2. Venkadesh KV, Setio AAA, Schreuder A, et al. Deep Learning for Malignancy Risk Estimation of Pulmonary Nodules Detected at Low-Dose Screening CT. Radiology 2021;300:438-47.
3. Chung KF, McGarvey L, Song WJ, et al. Cough hypersensitivity and chronic cough. Nat Rev Dis Primers 2022;8:45.
4. Yibrehu BA, Krakovsky GM, Rana MS, et al. Pediatric Quality-of-Life Scores Following a Multidisciplinary Aerodigestive Team Approach to Manage Chronic Cough. Ann Otol Rhinol Laryngol 2020;129:1088-94.
5. Hu XL, Xu ST, Wang XC, et al. Status of coexisting chronic obstructive pulmonary disease and its clinicopathological features in patients undergoing lung cancer surgery: a cross-sectional study of 3,006 cases. J Thorac Dis 2018;10:2403-11.
6. Sun H, Patil MJ, Ru F, et al. K(V) 1/D-type potassium channels inhibit the excitability of bronchopulmonary vagal afferent nerves. J Physiol 2022;600:2953-71.
7. Chou YL, Mori N, Canning BJ. Opposing effects of bronchopulmonary C-fiber subtypes on cough in guinea pigs. Am J Physiol Regul Integr Comp Physiol 2018;314:R489-98.
8. Gao X, Zhuang J, Zhao L, et al. Cross-effect of TRPV1 and EP3 receptor on coughs and bronchopulmonary C-neural activities. PLoS One 2021;16:e0246375.
9. Brozmanova M, Buday T, Konarska M, et al. The effect of the voltage-gated sodium channel Na(V)1.7 blocker PF-05089771 on cough in the guinea pig. Respir Physiol Neurobiol 2022;299:103856.
10. Liu M, Jia X, Liu H, et al. Role of TRPV1 in respiratory disease and association with traditional Chinese medicine: A literature review. Biomed Pharmacother 2022;155:113676.
11. Zhu YF, Wu SB, Zhou MQ, et al. Increased expression of TRPV1 in patients with acute or chronic cough after lung cancer surgery. Thorac Cancer 2019;10:988-91.
12. Liviero F, Scarpa MC, De Stefani D, et al. Modulation of TRPV-1 by prostaglandin-E(2) and bradykinin changes cough sensitivity and autonomic regulation of cardiac rhythm in healthy subjects. Sci Rep 2020;10:15163.
13. Gokhale M, Girman C, Chen Y, et al. Comparison of diagnostic evaluations for cough among initiators of angiotensin converting enzyme inhibitors and angiotensin receptor blockers. Pharmacoepidemiol Drug Saf 2016;25:512-20.
14. Okazaki A, Hara J, Ohkura N, et al. Role of prostaglandin E(2) in bronchoconstriction-triggered cough response in guinea pigs. Pulm Pharmacol Ther 2018;48:62-70.
15. Cong W, Peng Y, Meng B, et al. The effect of electroacupuncture on regulating pain and depression-like behaviors induced by chronic neuropathic pain. Ann Palliat Med 2021;10:104-13.
16. Xu Q, Niu C, Li J, et al. Electroacupuncture alleviates neuropathic pain caused by spared nerve injury by promoting AMPK/mTOR-mediated autophagy in dorsal root ganglion macrophage. Ann Transl Med 2022;10:1341.
17. Coyle ME, Shergis JL, Huang ET, et al. Acupuncture therapies for chronic obstructive pulmonary disease: a systematic review of randomized, controlled trials. Altern Ther Health Med 2014;20:10-23.
18. Xu YQ, Cui X, Liu K, et al. Comparison of effects of routine electroacupuncture and pre-electroacupuncture in improving lung function in acute lung injury rats. Acupuncture Research 2022;47:580-6.
19. Tu H, Zhang Q. Assessment of Acupoint Therapy of Traditional Chinese Medicine on Cough Variant Asthma: A Meta-analysis. Biomed Res Int 2022;2022:4168308.
20. Chen YM, Xie XL, Xiao PY, et al. Acupuncture on treating asthma: A protocol for systematic review and meta analysis. Medicine (Baltimore) 2020;99:e18457.
21. Levy I, Elimeleh Y, Gavrieli S, et al. Treatment of acute exacerbations of chronic obstructive pulmonary disease with acupuncture during hospitalization: a three-arm double-blinded randomized sham-controlled trial. Acupunct Med 2022;40:505-15.
22. Zhu YF, Xie MR, Zhou MQ. Establishment of Cough Model after Guinea Pig Lung Resection and the Effect of Acupuncture Lung Meridian on its Serum of PGE-2 and BK. Clinical Journal of Traditional Chinese Medicine 2019;31:294-7.
23. Huang Y, Lu SF, Hu CJ, et al. Electro-acupuncture at Neiguan pretreatment alters genome-wide gene expressions and protects rat myocardium against ischemia-reperfusion. Molecules 2014;19:16158-78.
24. Ren LQ, Li C, Shi Y. Animal model of cough. Replication of the animal models for human diseases. Beijing: People's Medical Publishing House; 2008:17-4.
25. Wu XM, Bian RL. Antitussive drug experiment method.

Pharmacological experimental methodology. 3 Edition. Beijing: People's Medical Publishing House; 2002:1362-6.
26. Keller SM, Adak S, Wagner H, et al. Mediastinal lymph node dissection improves survival in patients with stages II and IIIa non-small cell lung cancer. Eastern Cooperative Oncology Group. Ann Thorac Surg 2000;70:358-65; discussion 365-6.
27. Lin R, Che G. Risk factors of cough in non-small cell lung cancer patients after video-assisted thoracoscopic surgery. J Thorac Dis 2018;10:5368-75.
28. Miyamoto H, Sakao Y, Sakuraba M, et al. Usefulness of suplatast tosilate for chronic cough following lung cancer surgery. Gen Thorac Cardiovasc Surg 2009;57:463-6.
29. Shelhamer JH, Levine SJ, Wu T, et al. NIH conference. Airway inflammation. Ann Intern Med 1995;123:288-304.
30. Hollenhorst MI, Nandigama R, Evers SB, et al. Bitter taste signaling in tracheal epithelial brush cells elicits innate immune responses to bacterial infection. J Clin Invest 2022;132:e150951.
31. Zhu X, Li H, Zhu TM, et al. Acupuncture combined with smokeless or smoky moxibustion for regulating immune function of experimental chronic rhinosinusitis mice. Acupuncture Research 2021;46:757-62.
32. Grace M, Birrell MA, Dubuis E, et al. Transient receptor potential channels mediate the tussive response to prostaglandin E2 and bradykinin. Thorax 2012;67:891-900.
33. Frey E, Karney-Grobe S, Krolak T, et al. TRPV1 Agonist, Capsaicin, Induces Axon Outgrowth after Injury via Ca(2+)/PKA Signaling. eNeuro 2018;5:ENEURO.0095-18.2018.
34. Bahia PK, Hadley SH, Barannikov I, et al. Antimycin A increases bronchopulmonary C-fiber excitability via protein kinase C alpha. Respir Physiol Neurobiol 2020;278:103446.
35. Ma W, St-Jacques B, Rudakou U, et al. Stimulating TRPV1 externalization and synthesis in dorsal root ganglion neurons contributes to PGE2 potentiation of TRPV1 activity and nociceptor sensitization. Eur J Pain 2017;21:575-93.
36. Del Fiacco M, Quartu M, Boi M, et al. TRPV1, CGRP and SP in scalp arteries of patients suffering from chronic migraine. J Neurol Neurosurg Psychiatry 2015;86:393-7.
37. Silberstein SD. TRPV1, CGRP and SP in scalp arteries of patients suffering from chronic migraine. Some like it hot! Chronic migraine increases TRPV1 receptors in the scalp. J Neurol Neurosurg Psychiatry 2015;86:361.

Cite this article as: Wang GX, Zhou J, Chen YM, Xu LD, Tao SM, Ma J, Sun YH, Wu MS, Chen ZW, Zhu YF, Xie MR. Mechanism of electroacupuncture at acupoints of the lung meridian through PKA/PKC regulation of TRPV1 in chronic cough after lung surgery in guinea pigs. J Thorac Dis 2023;15(4):1848-1860. doi: 10.21037/jtd-23-409

Supplementary

Table S1 Genetic testing using primer sequences

Gene	Primer	Sequence (5'-3')	PCR products
β-actin	Forward	*CACGATGGAGGGGCCGGACTCATC*	240bp
	Reverse	*TAAAGACCTCTATGCCAACACAGT*	
Cavia porcellus NK1R	Forward	*CTGCGGTCTTTGCCAGTATC*	171bp
	Reverse	*TGGTTGAGTAGTAGCCCTGC*	
Cavia porcellus TRPV1	Forward	*CAGTGGGAAGATTGGGGTCT*	207bp
	Reverse	*TCATGGCGATTAGGGGTCTC*	
Cavia porcellus SP	Forward	*CGGAGGAAAACACAGCCATT*	240bp
	Reverse	*ACTCACAGATGGTCAGTCGG*	
Cavia porcellus CGRP	Forward	*CGAAGGACTCTAGCTCACCG*	193bp
	Reverse	*CCAGGTCTAGGCTGTTGTCT*	

Table S2 Comparison of cough in each group

Test details	Mean 1 (times/6 min)	Mean 2(times/6 min)	P value
Sham *vs.* Model	2.5	15.67	<0.0001
Sham *vs.* EA + M	2.5	7.5	0.0002
Sham *vs.* H89 + M	2.5	9.167	<0.0001
Sham *vs.* Go6983 + M	2.5	9.5	<0.0001
Model *vs.* EA + M	15.67	7.5	<0.0001
Model *vs.* H89 + M	15.67	9.167	<0.0001
Model *vs.* Go6983 + M	15.67	9.5	<0.0001
EA + M *vs.* H89 + M	7.5	9.167	0.9383
EA + M *vs.* Go6983 + M	7.5	9.5	0.4693
H89 + M *vs.* Go6983 + M	9.167	9.5	>0.9999

https://dx.doi.org/10.21037/jtd-23-409

Table S3 PGE2, BK, and TRPV1 protein expression in the bronchoalveolar lavage fluid and blood was determined by ELISA

Sample	Index	Test details	Mean 1	Mean 2	P Value
BALF	PGE2 (pg/mL)	Sham *vs.* Model	73.3	105.7	0.0001
		Sham *vs.* EA + M	73.3	85.23	0.584
		Sham *vs.* H89 + M	73.3	82	>0.9999
		Sham *vs.* Go6983 + M	73.3	82.89	>0.9999
		Model *vs.* EA + M	105.7	85.23	0.0226
		Model *vs.* H89 + M	105.7	82	0.0058
		Model *vs.* Go6983 + M	105.7	82.89	0.0085
		EA + M *vs.* H89 + M	85.23	82	>0.9999
		EA + M *vs.* Go6983 + M	85.23	82.89	>0.9999
		H89 + M *vs.* Go6983 + M	82	82.89	>0.9999
	BK (ng/mL)	Sham *vs.* Model	1.265	1.368	0.0152
		Sham *vs.* EA + M	1.265	1.225	>0.9999
		Sham *vs.* H89 + M	1.265	1.208	0.6371
		Sham *vs.* Go6983 + M	1.265	1.215	>0.9999
		Model *vs.* EA + M	1.368	1.225	0.0005
		Model *vs.* H89 + M	1.368	1.208	0.0001
		Model *vs.* Go6983 + M	1.368	1.215	0.0002
		EA + M *vs.* H89 + M	1.225	1.208	>0.9999
		EA + M *vs.* Go6983 + M	1.225	1.215	>0.9999
		H89 + M *vs.* Go6983 + M	1.208	1.215	>0.9999
	TRPV 1 (ng/mL)	Sham *vs.* Model	0.6565	1.307	0.0009
		Sham *vs.* EA + M	0.6565	0.6038	>0.9999
		Sham *vs.* H89 + M	0.6565	0.626	>0.9999
		Sham *vs.* Go6983 + M	0.6565	0.6113	>0.9999
		Model *vs.* EA + M	1.307	0.6038	0.0003
		Model *vs.* H89 + M	1.307	0.626	0.0005
		Model *vs.* Go6983 + M	1.307	0.6113	0.0004
		EA + M *vs.* H89 + M	0.6038	0.626	>0.9999
		EA + M *vs.* Go6983 + M	0.6038	0.6113	>0.9999
		H89 + M *vs.* Go6983 + M	0.626	0.6113	>0.9999
Blood	PGE2 (pg/mL)	Sham *vs.* Model	143.7	172.9	0.0098
		Sham *vs.* EA + M	143.7	137.9	>0.9999
		Sham *vs.* H89 + M	143.7	142.1	>0.9999
		Sham *vs.* Go6983 + M	143.7	138	>0.9999
		Model *vs.* EA + M	172.9	137.9	0.0014
		Model *vs.* H89 + M	172.9	142.1	0.0058
		Model *vs.* Go6983 + M	172.9	138	0.0015
		EA + M *vs.* H89 + M	137.9	142.1	>0.9999
		EA + M *vs.* Go6983 + M	137.9	138	>0.9999
		H89 + M *vs.* Go6983 + M	142.1	138	>0.9999
	BK (ng/mL)	Sham *vs.* Model	10.28	21.64	0.0016
		Sham *vs.* EA + M	10.28	13.06	0.8184
		Sham *vs.* H89 + M	10.28	11.98	0.9639
		Sham *vs.* Go6983 + M	10.28	11.82	0.9746
		Model *vs.* EA + M	21.64	13.06	0.0213
		Model *vs.* H89 + M	21.64	11.98	0.0079
		Model *vs.* Go6983 + M	21.64	11.82	0.0068
		EA + M *vs.* H89 + M	13.06	11.98	0.9933
		EA + M *vs.* Go6983 + M	13.06	11.82	0.9887
		H89 + M *vs.* Go6983 + M	11.98	11.82	>0.9999
	TRPV 1 (ng/mL)	Sham *vs.* Model	1.445	2.91	<0.0001
		Sham *vs.* EA + M	1.445	1.832	0.7439
		Sham *vs.* H89 + M	1.445	2.002	0.1286
		Sham *vs.* Go6983 + M	1.445	1.818	0.8481
		Model *vs.* EA + M	2.91	1.832	0.0002
		Model *vs.* H89 + M	2.91	2.002	0.0019
		Model *vs.* Go6983 + M	2.91	1.818	0.0002
		EA + M *vs.* H89 + M	1.832	2.002	>0.9999
		EA + M *vs.* Go6983 + M	1.832	1.818	>0.9999
		H89 + M *vs.* Go6983 + M	2.002	1.818	>0.9999

https://dx.doi.org/10.21037/jtd-23-409

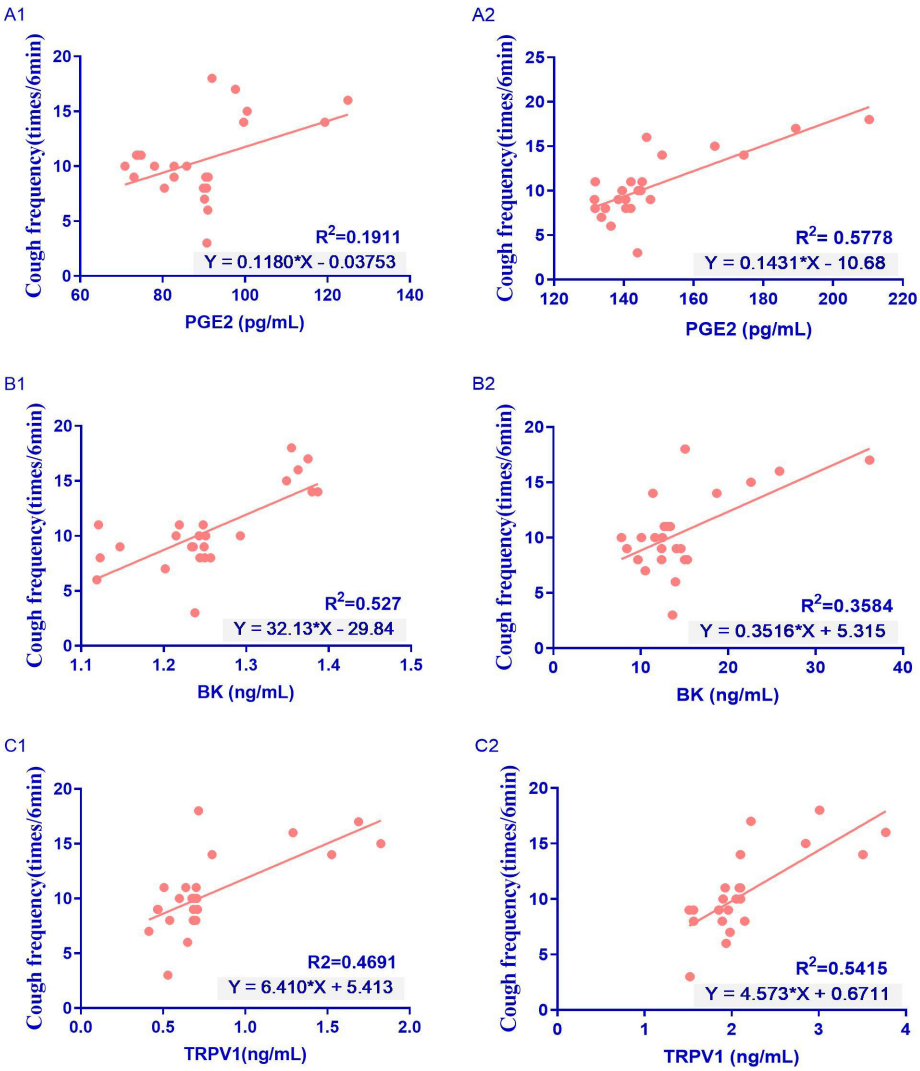

Figure S1 Correlation analysis of postoperative chronic cough in guinea pigs with the expression of PGE2, BK, TRPV1 in alveolar lavage fluid and blood.

https://dx.doi.org/10.21037/jtd-23-409

Table S4 Western blot Quantitative analysis of p-PKA, p-PKC, and p-TRPV1 protein expression in guinea-pig lung tissues

Index	Test details	Mean 1	Mean 2	P value
p-PKA	Sham *vs.* Model	0.6525	0.8552	0.0015
	Sham *vs.* EA + M	0.6525	0.522	0.0817
	Sham *vs.* H89 + M	0.6525	0.3512	<0.0001
	Sham *vs.* Go 6983 + M	0.6525	0.8118	0.0173
	Model *vs.* EA + M	0.8552	0.522	<0.0001
	Model *vs.* H89 + M	0.8552	0.3512	<0.0001
	Model *vs.* Go 6983 + M	0.8552	0.8118	>0.9999
	EA + M *vs.* H89 + M	0.522	0.3512	0.0091
	EA + M *vs.* Go 6983 + M	0.522	0.8118	<0.0001
	H89 + M *vs.* Go 6983 + M	0.3512	0.8118	<0.0001
p-PKC	Sham *vs.* Model	0.5087	0.7743	<0.0001
	Sham *vs.* EA + M	0.5087	0.5087	>0.9999
	Sham *vs.* H89 + M	0.5087	0.7905	<0.0001
	Sham *vs.* Go 6983 + M	0.5087	0.3387	0.0158
	Model *vs.* EA + M	0.7743	0.5087	<0.0001
	Model *vs.* H89 + M	0.7743	0.7905	>0.9999
	Model *vs.* Go 6983 + M	0.7743	0.3387	<0.0001
	EA + M *vs.* H89 + M	0.5087	0.7905	<0.0001
	EA + M *vs.* Go 6983 + M	0.5087	0.3387	0.0158
	H89 + M *vs.* Go 6983 + M	0.7905	0.3387	<0.0001
p-TRPV 1	Sham *vs.* Model	0.7482	0.9845	0.0082
	Sham *vs.* EA + M	0.7482	0.5412	0.0269
	Sham *vs.* H89 + M	0.7482	0.5395	0.0252
	Sham *vs.* Go 6983 + M	0.7482	0.5335	0.0198
	Model *vs.* EA + M	0.9845	0.5412	<0.0001
	Model *vs.* H89 + M	0.9845	0.5395	<0.0001
	Model *vs.* Go 6983 + M	0.9845	0.5335	<0.0001
	EA + M *vs.* H89 + M	0.5412	0.5395	>0.9999
	EA + M *vs.* Go 6983 + M	0.5412	0.5335	>0.9999
	H89 + M *vs.* Go 6983 + M	0.5395	0.5335	>0.9999

https://dx.doi.org/10.21037/jtd-23-409

Table S5 TRPV1, SP, CGRP, and NK1R mRNA content were measured in guinea pig lung tissue by quantitative real-time lung PCR analysis

Index	Test details	Mean 1	Mean 2	P Value
TRPV1 mRNA	Sham *vs.* Model	1.403	2.265	0.0113
	Sham *vs.* EA + M	1.403	1.463	>0.9999
	Sham *vs.* H89 + M	1.403	0.9627	0.0275
	Sham *vs.* Go 6983 + M	1.403	0.577	0.0176
	Model *vs.* EA + M	2.265	1.463	0.0055
	Model *vs.* H89 + M	2.265	0.9627	0.0004
	Model *vs.* Go 6983 + M	2.265	0.577	0.0001
	EA + M *vs.* H89 + M	1.463	0.9627	0.1583
	EA + M *vs.* Go 6983 + M	1.463	0.577	0.016
	H89 + M *vs.* Go 6983 + M	0.9627	0.577	0.6182
SP mRNA	Sham *vs.* Model	1.419	2.291	0.0029
	Sham *vs.* EA + M	1.419	1.096	>0.9999
	Sham *vs.* H89 + M	1.419	0.812	0.0708
	Sham *vs.* Go 6983 + M	1.419	0.5108	0.0018
	Model *vs.* EA + M	2.291	1.096	<0.0001
	Model *vs.* H89 + M	2.291	0.812	<0.0001
	Model *vs.* Go 6983 + M	2.291	0.5108	<0.0001
	EA + M *vs.* H89 + M	1.096	0.812	>0.9999
	EA + M *vs.* Go 6983 + M	1.096	0.5108	0.091
	H89 + M *vs.* Go 6983 + M	0.812	0.5108	>0.9999
CGRP mRNA	Sham *vs.* Model	1.131	2.387	<0.0001
	Sham *vs.* EA + M	1.131	1.381	0.8325
	Sham *vs.* H89 + M	1.131	0.9162	>0.9999
	Sham *vs.* Go 6983 + M	1.131	0.7692	0.1535
	Model *vs.* EA + M	2.387	1.381	<0.0001
	Model *vs.* H89 + M	2.387	0.9162	<0.0001
	Model *vs.* Go 6983 + M	2.387	0.7692	<0.0001
	EA + M *vs.* H89 + M	1.381	0.9162	0.0258
	EA + M *vs.* Go 6983 + M	1.381	0.7692	0.0017
	H89 + M *vs.* Go 6983 + M	0.9162	0.7692	>0.9999
NK1R mRNA	Sham *vs.* Model	1.183	1.745	0.0238
	Sham *vs.* EA + M	1.183	0.873	0.4225
	Sham *vs.* H89 + M	1.183	0.8997	0.7732
	Sham *vs.* Go 6983 + M	1.183	0.5525	0.0013
	Model *vs.* EA + M	1.745	0.873	0.0049
	Model *vs.* H89 + M	1.745	0.8997	0.03
	Model *vs.* Go 6983 + M	1.745	0.5525	0.0002
	EA + M *vs.* H89 + M	0.873	0.8997	>0.9999
	EA + M *vs.* Go 6983 + M	0.873	0.5525	0.1909
	H89 + M *vs.* Go 6983 + M	0.8997	0.5525	0.7072

https://dx.doi.org/10.21037/jtd-23-409